Experimentally-Derived Phase Function Approximations in Support of the Orbital Debris Program Office

J. Hostetler[(1)] and H. Cowardin[(1)]

[(1)]Jacobs, NASA Johnson Space Center, 2224 Bay Area Blvd, Houston, TX 77058, john.m.hostetler@nasa.gov

ABSTRACT

The NASA Orbital Debris Program Office (ODPO) has used various optical assets to acquire photometric data of Earth-orbiting objects to define the orbital debris environment. To better characterize and model optical data acquired from ground-based telescopes, the Optical Measurements Center (OMC) at NASA Johnson Space Center emulates illumination conditions seen in space by using equipment and techniques that parallel telescopic observations and source-target-sensor orientations.

One of the OMC goals is to improve the size calculation used for optical data by developing an optical-based Size Estimation Model. The current size estimation requires applying a Lambertian phase function, a set albedo value, and range to the observed magnitude. The first step to improving the sampled brightness of laboratory targets is to remove aspect-angle dependencies. Then, the volume of possible object viewing angles is sampled at 21 combinations of azimuth and elevation angles for each solar phase angle. Finally, the acquired images are input into an image processing program that generates approximations for the object's Bidirectional Reflectance Distribution Function (BRDF) and phase function. The BRDF is a radiometric concept that identifies an object's material composition by matching a BRDF approximated with photometric data collected by ground-based telescopes with a BRDF generated experimentally from a known object in the laboratory.

This paper presents the initial BRDF and phase function approximations for various fragments/targets acquired in the OMC and how the findings will be incorporated into ODPO models. A Lambertian sphere is used as a baseline for initial size estimation calculations and phase function comparisons. Spacecraft materials and fragments from hypervelocity laboratory impact tests are also presented to compare against the current assumed Lambertian phase function used for size estimates. This paper presents the preliminary phase function analysis and plan forward to utilize a laboratory-based phase function to improve the current optical size estimates using BRDF measurements for a large volume of targets composed of various shapes, sizes, and materials.

1 INTRODUCTION

The NASA Orbital Debris Program Office (ODPO) has utilized optical observations of Earth-orbiting objects to better characterize the orbital debris environment. Ground-based measurements provide time-dependent orbital parameters and brightness (i.e., magnitudes). The magnitude data is converted into size assuming a range, phase function, and albedo. Capitalizing on optical data products, using laboratory measurements acquired in the Optical Measurements Center (OMC) and applying them to generate a more complete understanding of orbital space objects is a key objective of NASA's Optical Measurements Program. The OMC is used to emulate space-based illumination conditions using equipment and techniques that parallel telescopic observations and source-target-sensor orientations.

The ground-based optical data collected to date is used as direct inputs into NASA's Orbital Debris Engineering Model (ORDEM), providing the orbital elements of each detection and its estimated size. To improve upon the current size estimation, the OMC is investigating new phase functions based on spacecraft material samples and fragments from laboratory hypervelocity impact tests, with plans to generate a distribution of phase functions. In addition, the fragments from a recent hypervelocity test, DebriSat, provided 3-D-point clouds of fragments, which are used to calculate a size (characteristic length) that is used to directly compare to the optical size estimates. The characteristic length is defined as the average of the largest dimensions for an object measured along three orthogonal axes. The first axis coincides with the largest dimension, the second axis is in a plane orthogonal to the first axis, and the third axis is chosen to complete the orthogonal triad.

The following presents the latest results of a baseline Lambertian sphere and four targets that provide an initial assessment of the empirical-based phase functions. Utilizing the laboratory Bidirectional Reflectance Distribution

Function (BRDF) measurements removes any aspect angle dependence, and thus initial size estimates are presented based on known size estimates from a DebriSat fragment. The research goal is to refine the optical size estimation model using known fragments from laboratory tests to compare with ground-based optical data to improve our environmental and engineering models.

2 DATA ACQUISITION / INSTRUMENTATION

The OMC's design is analogous to a telescope set-up with a light source, target, and observer. A 75W, Xenon arc lamp simulates solar illumination from 200 nm to 2500 nm. The data are acquired through a Santa Barbara Instrument Group charge-coupled device (CCD) camera (1024 x 1536 pixels) with an attached filter wheel that uses the standard astronomical suite of Johnson/Bessell filters: Blue (B), Visible (V), Red (R), Clear (C) and Infrared (I). The laboratory equipment is capable of obtaining data for a full 360° range in phase angle (the vertex angle between light source, object, and detector) with an accuracy of 1° using a custom-built rotary arm with attached commercial off-the-shelf potentiometer. To prevent scattered light from biasing the observations, a light trap (not shown) is placed directly across from the light source on the other end of the rotary arm, therefore, the data is limited to phase angles between ±(3°- 160°). The layout is shown in Fig.1 with small digital images of the equipment. The target is oriented at the end of a robotic arm, recently improved with the addition of a sixth degree of freedom which enables the target to be viewed at any desired orientation. A 3D-printed polylactic acid end effector was also designed and implemented to eliminate as much interference as possible from light scattering off the robotic arm.

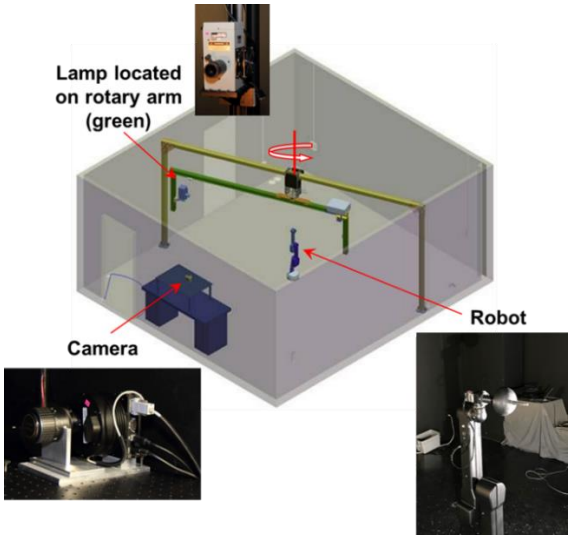

Fig. 1. OMC Experimental Setup [1].

The objective of this work is to improve the accuracy of size calculations used for optical data by developing an optical-based Size Estimation Model. The accepted approach in the approximation of orbital debris size, as developed by Barker, et al. [2], is a photometric determination utilizing both observable and assumed properties of the target. The principle observed parameter in this determination is the target's apparent brightness, or the apparent magnitude, m_{app}, which is a function of band pass, time, distance, and phase angle. For solar illuminated objects, m_{app} is dependent on the ratio of the observable flux, F_{app}, to the solar flux, $F_{sun,}$ in a given band pass (e.g., V, R, or I) [2].

$$m_{app}(v) - M_{sun}(v) = -2.5 \times \log\left[\frac{F_{app(v)}}{F_{sun}(v)}\right] \tag{1}$$

It is necessary to normalize this apparent brightness to a standard distance, R_o, because the apparent brightness of an object is proportional to the square of the distance from the Sun, R_{sun}, to the object, R. This normalization is done via the following relation [2]:

$$M_{abs}(v) = m_{app}(v) - 5.0 \times \log\left[\frac{R}{R_o}\right] - 5.0 \times \log\left[\frac{R_{sun}}{R_{sun}(1\ AU)}\right] \tag{2}$$

The observed flux, F_{app}, reflected from a target with an optical cross section (OCS) is given by Barker, et al. [2] as:

$$F_{app}(v) = OCS \times F_{sun}(v) = \Omega[\alpha_g f(\phi)] F_{sun}(v) = \frac{\pi d^2}{4R^2} \alpha_g f(\phi) F_{sun}(v) \tag{3}$$

where Ω is the solid angle subtended by the object with an OCS of diameter, d, at a given distance, R. The product of geometric albedo, α_g, of the object's surface, and the phase function, $f(\phi)$, represents the Bond albedo of the target, where α_g relates the actual brightness observed to that of an idealized flat, Lambertian disk or sphere with the same cross section, and $f(\phi)$ defines how sunlight is scattered by the surface in the direction ϕ to the observer. Utilizing Eq. (1) to define the ratio of F_{app} to F_{sun} in terms of absolute magnitude, $M_{abs}(v)$, and substituting this into the Eq. (3), it is then possible to solve for d:

$$d = \frac{2R}{\left[\pi \alpha_g f(\phi)\right]^{1/2}} \times 10^{\left[\frac{M_{abs}(\gamma) + M_{sun}(\gamma)}{-5}\right]} \tag{4}$$

To determine $M_{abs}(v)$ for an object in the OMC, the ratio of observable-to-solar flux is replaced with the illuminance ratio for a space object, defined by Hejduk, et al. [3] as:

$$\frac{E_r}{E} = \frac{k \alpha A}{R^2} f(\phi) \tag{5}$$

where E_r is the irradiance measured from the object, E is the corresponding irradiance of a Spectralon panel occupying the same spatial coordinates as the object, α is the Bond albedo of the object, and k is a constant specific to the observed shape (a.k.a. shape factor). By reformulating the illuminance ratio in terms of stellar magnitudes through the conversion

$$\Delta_{mag} = -2.5 \times \log_{10}\left[\frac{E_r}{E}\right] \tag{6}$$

it is then possible to create a parallel formulation for the absolute magnitude of the object by fixing the Sun as the illumination source [3]:

$$M_{abs}(v) = -26.74 + \Delta_{mag} \tag{7}$$

$$M_{abs}(v) = -26.74 + \Delta_{mag} = -26.74 - 2.5 \log_{10}\left[\frac{k \alpha A f(\phi)}{R^2}\right] + 5 \log_{10}(R) \tag{8}$$

Substituting Eq. (8) for Eq. (1) into Eq. (4) results in the following size estimation for objects measured in the OMC:

$$d_{OMC} = \frac{2R}{\left[\pi \alpha_g f(\phi)\right]^{1/2}} \times 10^{\left[\frac{-26.74 - 2.5 \cdot \log_{10}\left(\frac{E_r}{E}\right) + 5 \cdot \log_{10}(R)}{-5}\right]} \tag{9}$$

2.1 Phase Function Approximation

While many of the quantities used in the size estimation model are readily accessible via photometric analysis, the quantities α_g (geometric albedo) and $f(\phi)$ (phase function) are material dependent and thus approximations have been made to apply to the overall optical data products to derive size estimates. A geometric albedo of 0.175 is assumed for all objects, a value found to minimize the fractional error in resulting size estimations [4], and the phase function of orbital debris is assumed to be either Lambertian or specular, though it is well understood that for rocket bodies, spacecraft, and complex shapes the phase function is a complex combination of specular and Lambertian phase functions [2]. The Lambertian phase function is specified by Barker, et al. as

$$f(\phi) = \frac{2}{3\pi^2}\left[\sin(\phi) + (\pi - \phi)\cos(\phi)\right] \tag{10}$$

$$f(0) = 0.212207 \tag{11}$$

while the specular phase function, defined to be independent of phase angle, is given as

$$f(\phi) = \frac{1}{4\pi} \tag{12}$$

The resulting size estimation at a phase angle of ϕ=0° for an object using a specular phase function approximation is 161.2% larger than its Lambertian counterpart. This work therefore will endeavor to increase the accuracy of size estimations by generating an experimentally derived phase function in the OMC. E_r is determined for an object, and the Δ_{mag} of that object is subsequently approximated by measuring E from a flat-field image taken of a Spectralon panel, taken at the same spatial coordinates and using identical image acquisition parameters as those used with the object (*e.g.*, CCD filter, exposure time, etc.). The image intensity of the object is then scaled to the Lambertian phase function using Eq. (11) by determining the ratio of E_r to E at $f(\phi)$ = 0°.

3 DATA / RESULTS

3.1 Phase Function Approximation Qualification

The experimental phase function approximation process was initially qualified by sampling a 'Lambertian' sphere, which was found in previous studies to exhibit surface optical properties in close parody with those of a perfectly diffuse surface [5]. The Lambertian sphere, oriented at θ=0° and ψ=0°, was imaged with a Clear Johnson/Bessel filter, with a 1-second exposure time for each phase angle (ϕ) in a solar range of 5° to 155° in 5° increments (Fig. 2). As a result, no experimental BRDF measurements are presented in this work, as it was desired to first investigate the merit of utilizing an experimentally derived phase function at one view orientation before removing any aspect-angle dependencies in the size estimation model.

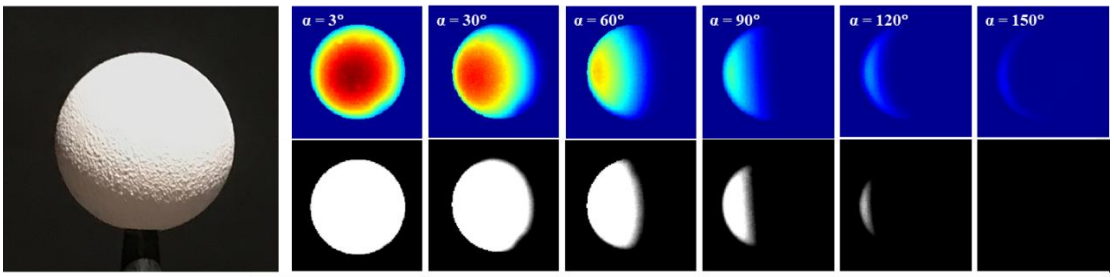

Fig. 2. (left) Lambertian sphere test object and (right) representative binary and color map renderings of captured images of Lambertian sphere across the solar range [5].

The irradiance of the object, E_r, was obtained by first summing the digital number corresponding to each bin in the CCD array after applying a binary mask to the image to isolate the object from the background. The resulting sum of counts in the image was then multiplied by the gain of the CCD and divided by the exposure time to determine the radiant flux. In a parallel computation, the pixels that were active in the binary mask were summed and multiplied by the pixel width and height to approximate the area which the object occupies on the CCD array, and the diameter of a circle with an equivalent area is determined. The re-distribution of the area to make it circular was done because most spacecraft and debris are un-resolved when observed from the ground with a telescope, and in effect act as a point source of light. The approximated diameter of the assumed circular object was subsequently used in conjunction with the measured radiant flux to approximate the irradiance. This calculation was then repeated with an image of the Spectralon panel to determine E.

The irradiance ratio between the Lambertian sphere and the Spectralon panel was found to be consistently equal to 3/5. Given that both the Lambertian sphere and Spectralon panel were both strongly diffuse, it was surmised that this ratio constituted the shape factor in Eq. (5) for a flat panel. Therefore, the irradiance of the Spectralon panel was normalized by this factor of 0.6 for all subsequent measurements. The resulting phase function approximation for the Lambertian sphere is plotted alongside the theoretical Lambertian and specular phase function assumptions in Fig. 3. While the experimental and theoretical Lambertian phase functions do share some resemblance, the curve of the experimental phase function is slightly steeper than its theoretical counterpart, and the Δ_{mag} curves diverge significantly after a phase angle of ϕ=60°. This is possibly due to the minor imperfections in the Lambertian coated sphere versus a theoretical, perfectly diffuse sphere.

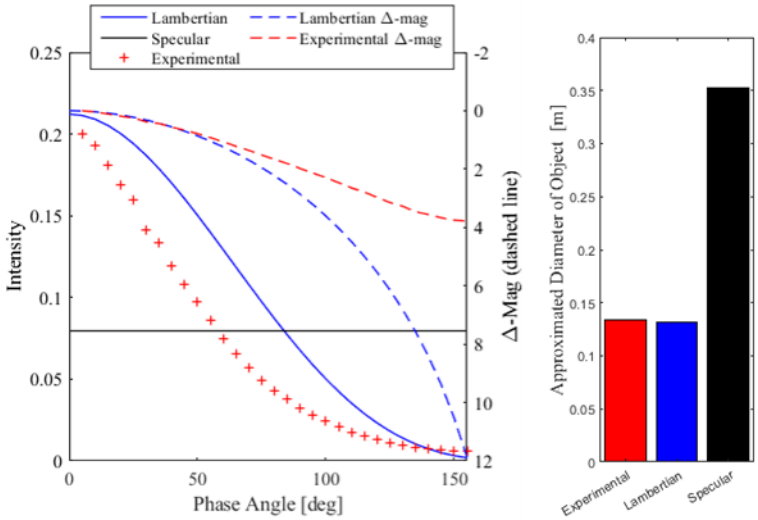

Fig. 3. (left) Phase functions generated for the Lambertian sphere test object and (right) comparative size estimations for *d* resulting from theoretical specular (blue), theoretical Lambertian (Lambertian), and experimental Lambertian phase functions (red).

The resulting size estimations made with the experimental and theoretical Lambertian phase functions, customarily made at ϕ=0°, are in close agreement while the specular assumption is much larger (Table 1.). However, given that the actual diameter of the Lambertian sphere was known to be 0.0381 m, even the more conservative Lambertian and experimental size estimations are still more than 2.5 times larger than truth when applying the assumed albedo value of 0.175 for α_g. When this assumed value is adjusted to that of a flat, perfectly diffuse surface multiplied by the shape factor of 3/5, the experimental size estimation becomes 0.0390 m – less than 2.4% from the true value. This residual error is likely due to imperfections on the sphere's surface, described in detail in previous work [5].

Table 1. Size estimations for Lambertian sphere with approximated values for geometric albedo and phase function

$\alpha_g = 0.175$	d [m]	% Error
Lambertian	0.1322	246.98
Specular	0.3525	825.20
Experimental	0.1338	251.18

$\alpha_g = 0.6$	d [m]	% Error
Lambertian	0.0386	1.31
Specular	0.1028	169.82
Experimental	0.039	2.36

3.2 Phase Function Approximations for Objects Representative of Orbital Debris

To better characterize the orbital debris environment using ground-based optical assets and to better understand the photometric data products for use in developing environmental models, a representation of fragments and materials are analyzed in the OMC. For this paper a focused selection on four representative targets were analyzed , θ=0° and ψ=0° using a Clear Johnson/Bessel filter with a 1-second exposure time for each phase angle in a solar range of 5° to 155° in 5° increments; their phase functions subsequently determined and used to estimate the size of the known objects. The first sample imaged was a small section of Carbon Fiber Reinforced Polymer (CFRP), a commonly used spacecraft material that serves multiple functions (Fig. 4).

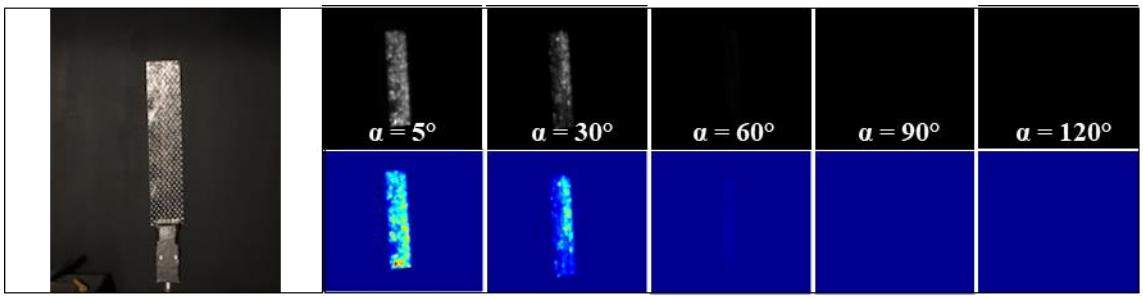

Fig. 4. (left)CFRP and (right) representative binary and color map renderings of CFRP across the solar range.

The resulting experimental size estimation was comparatively smaller than its Lambertian counterpart (Table 2). Despite the Lambertian estimation being almost double the actual dimension, both the Lambertian and experimental values were more accurate than the specular assumption, which estimated a value for *d* that was almost 7 times larger than truth.

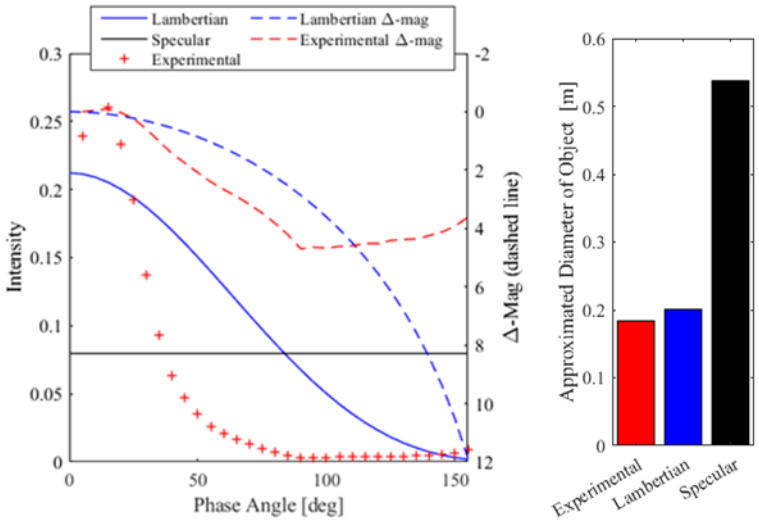

Fig. 5. (left) Phase functions generated for the CFRP and (right) comparative size estimations for *d* resulting from theoretical specular, theoretical Lambertian, and experimental Lambertian phase functions.

Table 2. Comparative Size Estimations for CFRP and Resulting Percentage Error

Model	*d* [m]	% Error
Lambertian	0.2013	194.3040
Specular	0.5368	684.8108
Experimental	0.183	167.5491

The phase function of the CFRP (Fig. 5) also demonstrates how other details of the object's shape (i.e., flat plate) may be inferred from the characteristics of the phase function. For instance, there is sharp decline in intensity over a subset of the solar range of 15°-50°, after which the intensity curve slowly decreases towards zero by ϕ=90°. Additionally, the Δ_{mag} curve increases in value until ϕ=90°, at which point the values become almost constant. These characteristics are indicative of a flat surface perpendicular to the observer – a behavior also exhibited by the intact multi-layered insulation (MLI) sample (Fig. 6-7). While the Δ_{mag} curve for the MLI initially remained close to zero, characteristic of a specular phase function, the Δ_{mag} also begins to dramatically decrease as the phase angle increases beyond 35°. Previous work presented by Hejduk, et al. [3] showed a correspondence in the diffuse/specular phase functions as a function of shape. The CFRP and MLI show consistencies with the cylindrical targets previously presented, suggesting that flat plates and cylinders may have overlaps in phase function characteristics.

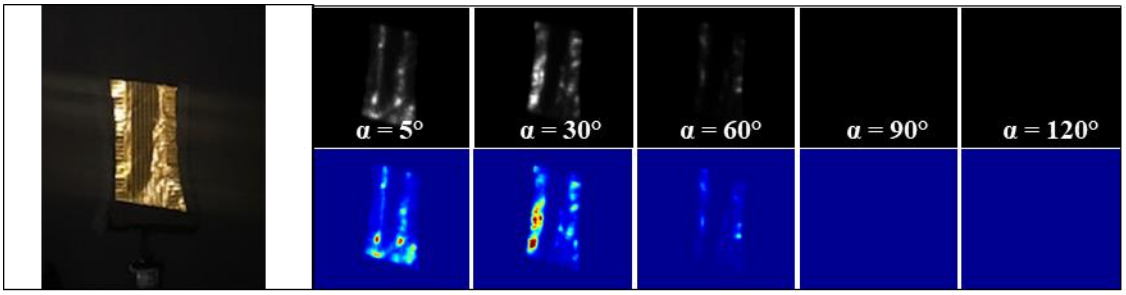

Fig. 6. (left)MLI and (right) representative binary and color map renderings of MLI across the solar range.

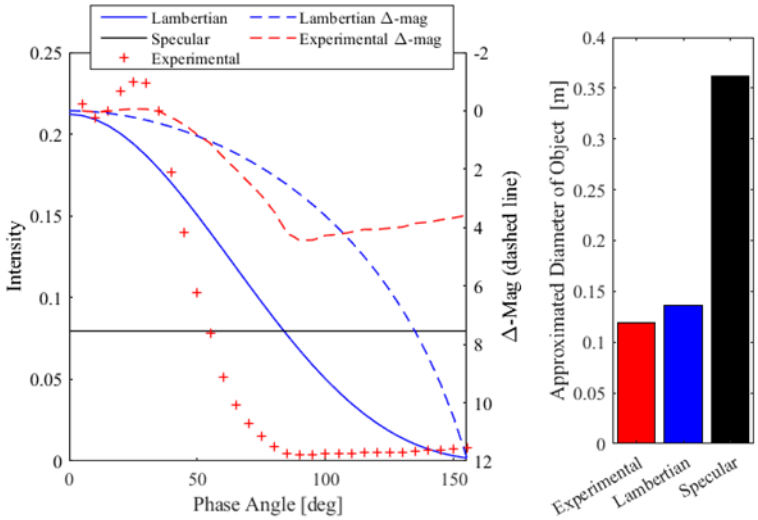

Fig. 7. (left) Phase functions generated for the MLI and (right) comparative size estimations for *d* resulting from theoretical specular, theoretical Lambertian, and experimental Lambertian phase functions.

The next imaged object, a telescope frame-cylindrical object, was one of the larger resultant fragments from the DebriSat experiment, a hypervelocity impact test using a high-fidelity mock-up satellite representative of present-day Low Earth Orbit (LEO) satellites. In addition to being an excellent example of orbital debris, this object was selected for analysis because it has known dimensions and a characteristic length determined from a point cloud analysis. This debris target was imaged in the OMC, oriented so as to present the X-Y plane of the object to the CCD (Fig. 8), and the resulting phase function was found to exhibit very low intensity values in comparison with the theoretical Lambertian and specular cases (Fig. 9).

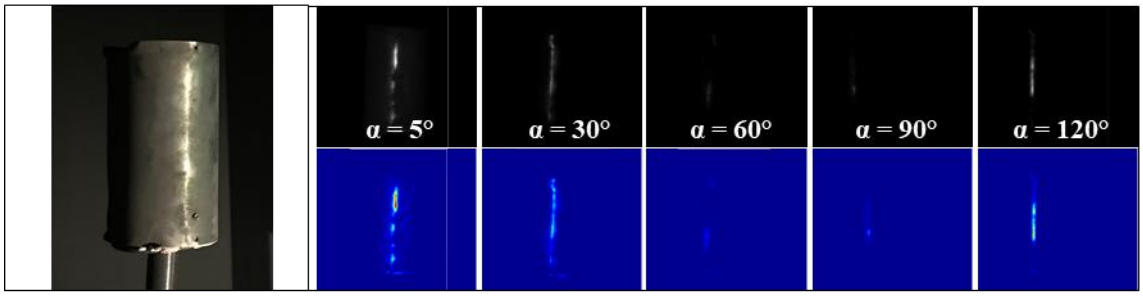

Fig. 8. (left) Telescope frame and (right) representative binary and color map renderings of images acquired throughout the solar range.

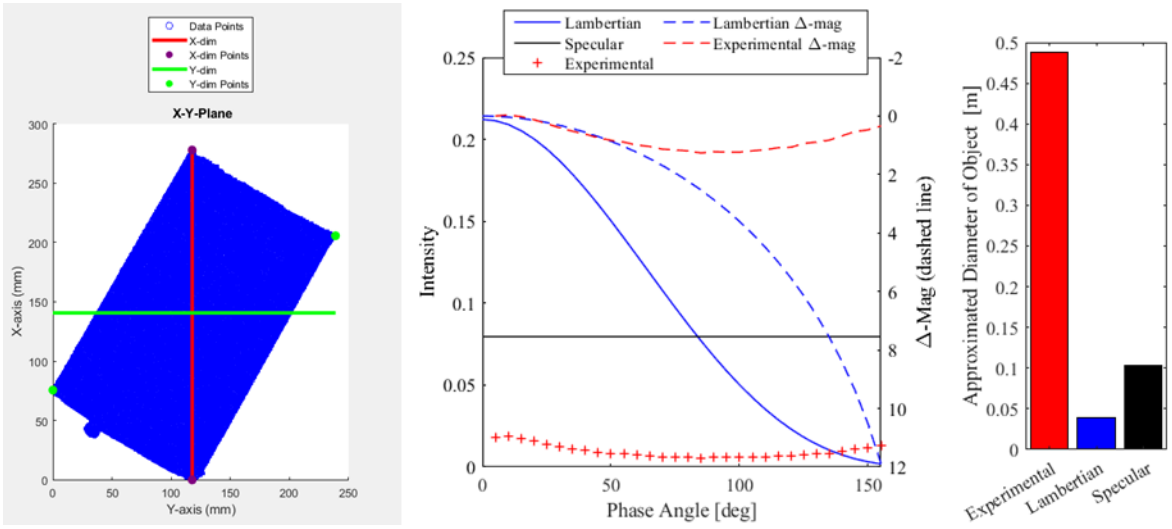

Fig. 9. (left) Point cloud analysis of X-Y Plane of telescope frame, (center) phase functions generated for the telescope frame, and (right) comparative size estimations for *d* resulting from theoretical specular, theoretical Lambertian, and experimental Lambertian phase functions.

The point cloud dimensional analysis for the X-Y plane of the telescope frame returned an actual value for surface area of 0.066378 m^2, but the resulting size estimations using the theoretical and experimental phase functions were varied and inaccurate (Table 3). This reiterates the dependency of accurate size estimations on the optical surface properties of the object itself. The surface of the debris was coated in a coarse black residue, likely due to the soft catch panels inside the impact chamber, which accorded a matte appearance to an already specular surface, further decreasing the observed radiant flux. Compounding this was that this object, in particular, has a large surface area – an order of magnitude larger than the repository of other objects sampled in this work. This combination of a matte specular surface with a large surface area resulted in a very low irradiance measurement, *E*, and subsequently may have contributed to the erroneously large estimation for the diameter of the OCS.

However, perhaps the most significant source of error in these results is that these size estimations are made in conjunction with an assumed geometric albedo of 0.175. The finding that the true size of the telescope frame lies between the specular and experimental estimations, in conjunction with the matte surface of the object itself, suggests that this assumed geometric albedo may contribute a significant amount to the egregious errors in the subsequent size estimations. Using the known diameter of the X-Y plane of the telescope frame of 0.2907 m with the experimentally determined phase function, the true geometric albedo of the frame was determined to be 0.3042 via Eq. (9). Using this determined value of α_g in the Lambertian and specular phase function size estimations resulted in the error increasing for both models. This finding suggests that utilizing either an experimentally determined phase function or geometric albedo alone will not suffice to ensure that the accuracy of subsequent size estimations will improve.

Table 3. Comparative Size Estimations for Telescope Frame

$\alpha_g = 0.175$	d [m]	% Error
Lambertian	0.0392	86.52
Specular	0.1045	64.05
Experimental	0.4919	69.20

$\alpha_g = 0.3042$	d [m]	% Error
Lambertian	0.0253	91.30
Specular	0.0675	76.78
Experimental	0.2907	0.00

This conclusion was later reinforced when a fragment was imaged from an earlier series of hypervelocity impact shots, called the Satellite Orbital Debris Characterization Impact Test (SOCIT) series conducted in the early 1990s. The SOCIT fragment (Fig. 10) has a very small surface area in comparison with the telescope frame; the resulting size estimation using the experimental phase function was similarly greater than its theoretical specular and Lambertian counterparts (Fig. 11), with a size estimation over 300% larger than the actual dimension (Table 4).

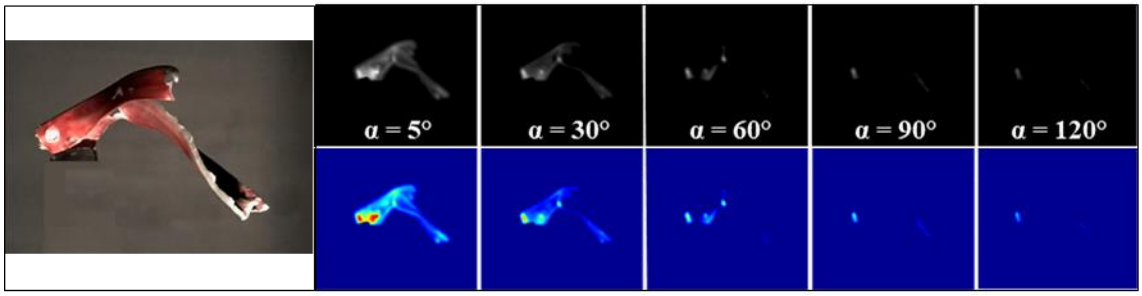

Fig. 10. (left) SOCIT fragment and (right) representative binary and color map renderings of images acquired throughout the solar range.

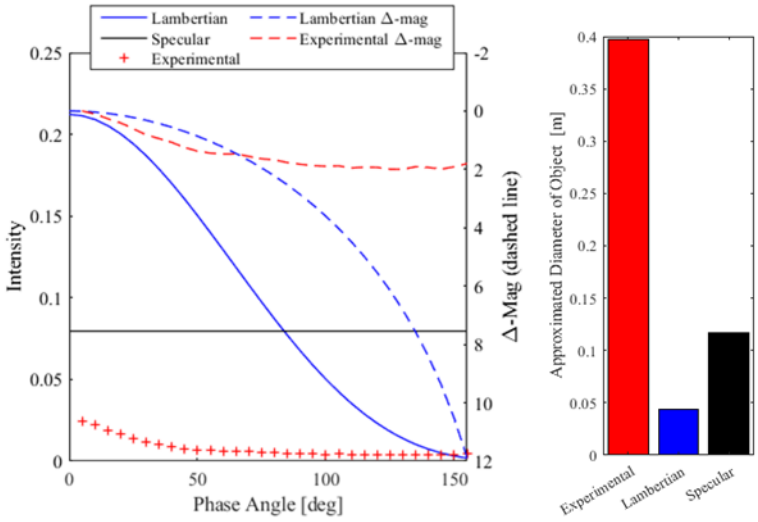

Fig. 11. (left) Phase functions generated for the SOCIT fragment and (right) comparative size estimations for *d* resulting from theoretical specular, theoretical Lambertian, and experimental Lambertian phase functions.

Perhaps the most noteworthy result from SOCIT fragment analysis is that the size estimations using specular and Lambertian assumptions were larger than those made previously for the telescope frame. Both theoretical size estimations for the SOCIT fragment were larger than those made for the telescope frame by exactly 12.24% – likely proportional to the ratios of observed M_{abs} between the two objects. By contrast, the size estimation obtained with the experimental phase function correctly indicates that the SOCIT fragment is smaller than the telescope frame, specifying a 19.3% reduction in surface area. While in reality the surface area of the telescope frame is more than 10 times greater than that of the SOCIT fragment, at least the experimental phase function does reflect the comparative size of one object to the other. Also, given that the surface of the SOCIT fragment is more diffuse than that of the telescope frame, the error in the size ratio, once again, likely is attributable to the application of a single assumed value of geometric albedo. The true geometric albedo for the fragment was determined to be 0.777, which when substituted into the size estimation model increases the error in the Lambertian and specular assumptions by ~40% (Table 4).

Table 4. Comparative Size Estimations for SOCIT fragment

$\alpha_g = 0.175$	d [m]	% Error
Lambertian	0.044	50.81
Specular	0.1173	31.13
Experimental	0.3969	343.70

$\alpha_g = 0.777$	d [m]	% Error
Lambertian	0.0099	88.93
Specular	0.0264	70.49
Experimental	0.0895	0.00

4 SUMMARY

The OMC has validated the experimentally derived phase function using a Lambertian sphere as a test object, and subsequently used this function to generate a size estimation for the sphere. The experimental size estimation agreed closely with the Lambertian assumption, but both results were more than twice the actual dimension of the sphere itself when the customary assumption that $\alpha_g = 0.175$ was applied. When the geometric albedo was adjusted to that of a perfectly-diffuse flat surface, and multiplied by the discovered shape factor of 3/5 between a disk and a sphere, the percent-error in the subsequent size estimations for the Lambertian assumption decreased to 1.31% and the experimental to 2.36%. The slightly larger error in the experimental assumption is likely due to surface imperfections on the imaged sphere itself which cause it not to act as a perfect Lambertian surface.

After validating the experimental phase function process, four objects with varying surface optical properties were imaged which were representative of orbital debris. The experimentally determined phase functions resulted in the most accurate size estimations for the CFRP and MLI, and the shapes of their phase functions demonstrated how certain aspects of the object's geometry may be inferred. Next, a large telescope frame was imaged, and the resulting estimations were erratic. The Lambertian and specular estimations were respectively 86.5% and 64% smaller than the true dimension, while the experimental phase function produced an estimation which was 69% too large. When the last object, a SOCIT fragment, was imaged, it was found that the size estimation using the experimental phase function was over three times too large, dwarfing its Lambertian and specular assumption counterparts.

Using the known size and experimentally determined phase function, the geometric albedo for each object was determined, and this value for α_g was then implemented in a second specular/Lambertian phase function size estimation. The experimentally determined values for geometric albedo were much larger than the assumed value of 0.175, likely inflated, in part, by the short distance between the object and the CCD, which created a much larger solid angle subtending the target. The comparative errors using both the assumed and experimentally determined values for α_g indicate that the experimental phase function is more sensitive to the geometric albedo than its specular and Lambertian counterparts, suggesting that while the OMC is capable of generating accurate phase functions experimentally, it should not be used in a size estimation unless it is accompanied by a simultaneously approximated value for geometric albedo. Therefore, future work involves developing a universal formula for the phase function, which includes coefficients that may be adjusted to fit measurements made for any observed body. Having done so, it may be possible to identify an unknown object by comparing a particular combination of these coefficients for an unknown object, observed via telescope, across a catalog of BRDFs for known objects analyzed experimentally in the OMC. In addition to identifying the object, the BRDF also would provide valuable insight into the orientation and/or tumble of the object and could be used to provide a supplementary approximation for geometric albedo as well.

5 REFERENCES

1. Cowardin, H., Mulrooney, M., Lederer, S., and Liou, J.-C. "Optical signature analysis of tumbling rocket bodies via laboratory measurements," 2012 AMOS Technical Conference, Maui, Hawaii, 11-14 September 2012.
2. Barker, E., *et al.* "Analysis of Working Assumptions in the Determination of Populations and Size Distributions of Orbital Debris from Optical Measurements," Proceedings of the 2004 AMOS Technical Conference, Wailea, Maui, HI, pp. 225-235, 2004.
3. Hejduk, M.D., Cowardin, H.M., and Stansbery, E.G. "Satellite Material Type and Phase Function. Determination in Support of Orbital Debris Size Estimation," 2012 AMOS Technical Conference, Maui, Hawaii, 11-14 September 2012.
4. Mulrooney, M., et al., "An Investigation of Global Albedo Values," 2008 AMOS Technical Conference, Maui, Hawaii, 16-19 September 2008.
5. Hostetler, J,M., Cowardin, H.M. "Experimentally-Derived Bidirectional Reflectance Distribution Function Data in Support of the Orbital Debris Program Office," 2019 AMOS Technical Conference, Maui, Hawaii.